2025 23rd European Control Conference (ECC)
June 24-27, 2025. Thessaloniki, Greece

Continuous-Time System Identification and OCV Reconstruction of Li-ion Batteries via Regularized Least Squares

Yang Wang, Riccardo M.G. Ferrari and Michel Verhaegen

Abstract— **Accurate identification of lithium-ion (Li-ion) battery parameters is essential for managing and predicting battery behavior. However, existing discrete-time methods hinder the estimation of physical parameters and face the fast-slow dynamics problem of the battery. In this paper, we develop a continuous-time approach that enables the estimation of battery parameters directly from sampled data. This method avoids discretization errors in converting continuous-time models into discrete-time ones. Moreover, the developed method is capable of jointly identifying the open-circuit voltage (OCV) and the state of charge (SOC) relation of batteries without utilizing offline OCV tests. By modeling the OCV-SOC curve as a cubic B-spline, we represent the piecewise nonlinearity of the OCV curve with high fidelity, facilitating its estimation. By solving a rank and L1 regularized least squares problem, we identify battery parameters and the OCV-SOC relation directly from the battery's dynamic data. Simulated and real-life data validate the effectiveness of the developed method.**

I. Introduction

Electric vehicles (EVs) have gained increasing attention owing to low-carbon policies and the appeal of sustainable transportation [1]. Lithium-ion (Li-ion) batteries are considered the most popular energy storage devices for EVs due to their favorable energy density, efficiency, and extended service life [2]. An accurate battery model is essential for reliable EV operation as it allows for an accurate prediction and management of the battery's performance.

Equivalent circuit models (ECMs) are battery models constructed with primary electrical elements. They are widely used in EVs because of their decent balance between accuracy and computational costs [3]. Current ECM identification mainly relies on discrete-time methods [4], [5]. Though directly manageable by digital computers, these approaches are inconvenient in estimating the physical parameters of the battery. Physical processes originally operate in continuous time, and discretization will introduce approximation errors, especially when the sampling time is incompatible with the time constants of the battery [6]. Moreover, batteries exhibit both fast and slow dynamics due to different polarization processes. This characteristic renders the discrete-time methods more challenging in identifying the battery's parameters [7].

Direct continuous-time identification allows for identifying a continuous-time model directly from sampled data without applying discretization [8]. From the identified continuous-time model, we can directly extract the physical parameters of the battery. The omission of discretization mitigates inefficiency and ill-conditioned problems in sampling stiff systems such as batteries, where both fast and slow dynamics are present [9]. This advantage benefits battery identification.

Identification of battery parameters presents another challenge in the nonlinear dependency between the open-circuit voltage (OCV) and the state of charge (SOC) of the battery [10]. The nonlinear characteristic renders conventional continuous-time methods not directly applicable to the ECM. To overcome this, an existing approach [11] measures OCV-SOC pairs via offline battery experiments and conducts linear system identification at individual SOC points with the continuous-time method. However, offline OCV tests are time-consuming and cannot be performed after the battery are installed on EVs, limiting their application [12]. A fractional-order model is developed by [13] to identify the battery parameters of a mobile robot. Though the OCV curve is identified from dynamic data, this method requires the time constants of the battery to be specified in advance and thus cannot reveal the actual battery parameters to provide physical interpretation.

In this paper, we develop a continuous-time method to jointly identify battery parameters and the OCV-SOC curve from sampled dynamic data of the battery. The OCV curve is modeled with a cubic B-spline to represent the piecewise nonlinearity of the OCV. Interaction between the dynamic parameters and the static OCV results in bilinear variables in the battery model. We utilize the low-rank property of a structured matrix of the bilinear variables to impose the bilinearity on the parameters in a linear least squares problem. With the constructed model, continuous-time identification is applied using a Laguerre filter bank that provides a more stable representation of the system than existing methods. By solving a rank and L1 regularized least squares problem, we simultaneously identify the continuous-time battery parameters and the OCV-SOC relation directly from the dynamic data of the battery.

Contributions: The contributions of this paper are summarized as follows:

- We develop a continuous-time method for identifying battery parameters;
- We formulate the OCV-SOC curve as a cubic B-spline for an enhanced OCV estimation;
- The battery parameters and the OCV-SOC relation are jointly identified by solving a rank and L1 regularized least squares problem;
- The effectiveness of the developed method is verified on a simulated battery and real-life data.

Yang Wang, Riccardo M.G. Ferrari, and Michel Verhaegen are with the Delft Center for Systems and Control, Delft University of Technology, Delft 2628CD, Netherlands. Email: {y.wang-40, r.ferrari, m.verhaegen}@tudelft.nl.

The rest of the paper is structured as follows. Section II introduces the equivalent circuit model for modeling Li-ion batteries. Section III describes the proposed continuous-time method for battery identification. Section IV verifies our method with a simulated battery and real-life battery data. Section V concludes the study and presents future work.

II. Lithium-ion Battery Model

Li-ion batteries can be modeled with a second-order equivalent circuit model (ECM) shown in Figure 1. The second-

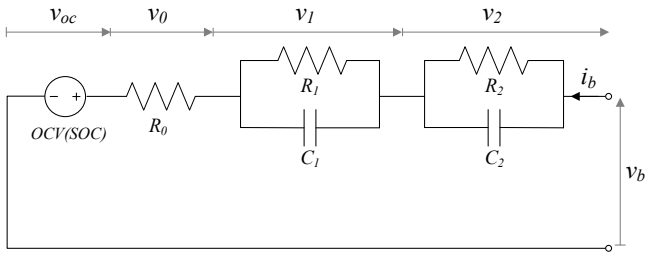

Fig. 1. Second-order equivalent circuit model

order ECM consists of an ohmic resistor R_0, two resistor-capacitor (RC) networks R_1C_1, R_2C_2, and an ideal voltage source v_{oc}. Resistor R_0 emulates the internal resistance of the battery, and the two RC networks represent the battery's fast and slow dynamics. Voltage source models the open-circuit voltage (OCV). Load current i_b and terminal voltage v_b are the model input and output, respectively. We define the charging direction as the positive direction of the current. The continuous-time state-space model of the ECM is as follows:

$$\begin{bmatrix}\dot{v}_1(t)\\ \dot{v}_2(t)\end{bmatrix} = \begin{bmatrix}-\frac{1}{R_1C_1} & 0\\ 0 & -\frac{1}{R_2C_2}\end{bmatrix}\begin{bmatrix}v_1(t)\\ v_2(t)\end{bmatrix} + \begin{bmatrix}\frac{1}{C_1}\\ \frac{1}{C_2}\end{bmatrix} i_b(t) \quad (1)$$

$$v_b(t) = \begin{bmatrix}1 & 1\end{bmatrix}\begin{bmatrix}v_1(t)\\ v_2(t)\end{bmatrix} + R_0 i_b(t) + v_{oc}(z(t)) + n_v(t), \quad (2)$$

where $v_1, v_2 \in \mathbb{R}$ are dynamic voltages across two RC circuits, $n_v(t) \in \mathbb{R}$ is the white measurement noise. The open-circuit voltage is a nonlinear function of the state of charge (SOC), which reveals the percentage of charges contained in the battery. The SOC, denoted by $z(t)$, can be calculated via Coulomb counting as:

$$z(t) = z(t_0) + \int_{t_0}^{t} \frac{1}{3600C} i_b(\tau) d\tau, \quad (3)$$

where $z(t_0)$ is the initial SOC at the time instant t_0, $C \in \mathbb{R}^+$ is the capacity of the battery in Ampere-hours (Ah), and the factor 3600 converts Ah into Coulombs.

To identify the battery parameters, we adopt the following assumptions about the input signal and the operating conditions of the battery:

Assumption 1 (Zero-order-hold input) *The input signal is generated by a zero-order-hold machine, and the sampling and the update of the input are synchronized exactly. The output is sampled at the same time as the input.*

Assumption 2 (Constant temperature and aging) *The ambient temperature of the battery is constant and does not change the battery's behavior, and the aging of the battery is considered zero during the identification.*

Assumption 3 (Constant battery parameters) *We assume battery parameters to be constant during charging and discharging.*

Assumption 1 can be adopted for batteries of EVs, where the input signal is generated by a digital microprocessor following a ZOH scheme. Synchronization between sampling and update ensures the input during the sampling interval has the same value as the previously sampled one. Assumption 2 excludes the influence of temperature and aging on the variation of battery parameters. Assumption 3 is adopted to maintain model simplicity and efficiency. This model has a lower computational cost while yielding sufficient accuracy for the typical SOC working range from 80% to 20%, where battery parameters present minimum variations [7], [10].

In this study, we aim to identify the battery parameters $R_i, C_j, i = 0, 1, 2, j = 1, 2$ of the ECM (1)(2) and the OCV-SOC relation of the battery $v_{oc}(z(t))$ from sampled input and output data of the battery.

III. Continuous-Time Battery Identification

In this section, we start with deriving a regression model of the ECM required by our continuous-time identification. Then, we introduce the cubic B-spline used to model the nonlinear OCV-SOC relation. Finally, a regularized least squares problem is formulated to identify the battery parameters and the OCV-SOC relation.

A. Regression model of the ECM with Laguerre filters

To conduct continuous-time identification of the battery, we write the state-space model (1)(2) into a continuous-time transfer function as:

$$G(s) = \frac{V_b(s) - V_{oc}(s)}{I_b} = \frac{b_0 s^2 + b_1 s + b_2}{s^2 + a_1 s + a_2}, \quad (4)$$

where s is the Laplace variable, and $V_b(s), I_b(s), V_{oc}(s)$ are the Laplace transforms of v_b, i_b and v_{oc}. The transfer function coefficients $a_i, b_j, i = 1, 2, j = 0, 1, 2$ are related to the ECM parameters with relations shown in (32). The transfer function (4) can be written into a linear equation as:

$$(s^2 + a_1 s + a_2)V_b(s) = (b_0 s^2 + b_1 s + b_2)I_b(s) + (s^2 + a_1 s + a_2)V_{oc}(s). \quad (5)$$

In continuous-time identification, derivatives of signals are not directly available from sampled data. To tackle this issue, we convert the transfer function into a Laguerre filter basis that captures the system's dynamics. Specifically, we use the Laguerre filter:

$$L_k(s) = \frac{2\nu}{s + \nu}\left(\frac{s - \nu}{s + \nu}\right)^k, \quad (6)$$

where $\nu \in \mathbb{R}_{>0}$ is the cut-off frequency, and $k = 0, 1, 2,$ is the order of the filter ranging from zero to the system order.

Using the Laguerre filter (6), the transfer function (5) can be converted into the following linear equation:

$$\begin{aligned}(\bar{a}_0 L_2(s) + \bar{a}_1 L_1(s) + \bar{a}_2 L_0(s))V_b(s) = \\ (\bar{b}_0 L_2(s) + \bar{b}_1 L_1(s) + \bar{b}_2 L_0(s))I_b(s) + \\ (\bar{a}_0 L_2(s) + \bar{a}_1 L_1(s) + \bar{a}_2 L_0(s))V_{oc}(s),\end{aligned} \quad (7)$$

where the transformed parameters $\bar{a}_i, \bar{b}_i, i = 0, 1, 2$ can be calculated from the original parameters in (5) and the cut-off frequency ν by the following relations:

$$\bar{a}_0 = \nu^2 - a_1\nu + a_2,\ \bar{a}_1 = 2\nu^2 - 2a_2, \quad (8)$$

$$\bar{a}_2 = \nu^2 + a_1\nu + a_2,\ \bar{b}_0 = b_0\nu^2 - b_1\nu + b_2, \quad (9)$$

$$\bar{b}_1 = 2b_0\nu^2 - 2b_2,\ \bar{b}_2 = b_0\nu^2 + b_1\nu + b_2. \quad (10)$$

Detailed derivations of (7) can be found in [8]. By applying the inverse Laplace transform to (7), we can write the linear equation into time domain as:

$$\begin{aligned}&\bar{a}_0[L_2 v_b](t) + \bar{a}_1[L_1 v_b](t) + \bar{a}_2[L_0 v_b](t) = \\ &\bar{b}_0[L_2 i_b](t) + \bar{b}_1[L_1 i_b](t) + \bar{b}_2[L_0 i_b](t) + \\ &\bar{a}_0[L_2 v_{oc}](z(t)) + \bar{a}_1[L_1 v_{oc}](z(t)) + \bar{a}_2[L_0 v_{oc}](z(t)),\end{aligned} \quad (11)$$

where

$$[L_k v_b](t) = l_k(t) * v_b(t) \quad (12)$$

$$[L_k i_b](t) = l_k(t) * i_b(t) \quad (13)$$

$$[L_k v_{oc}](z(t)) = l_k(t) * v_{oc}(z(t))\,, \quad (14)$$

and $*$ is the convolution operator and $l_k(t)$ is the impulse response of the Laguerre filter $L_k(s)$. From the time domain relation (11), we can write its regression form as:

$$\begin{aligned}[L_2 v_b](t) = \begin{bmatrix}-[L_{(1,0)} v_b](t) & [L_{(2,0)} i_b](t)\end{bmatrix}\begin{bmatrix}\tilde{a} \\ \tilde{b}\end{bmatrix} + \\ [L_2 v_{oc}](z(t)) + [L_{(1,0)} v_{oc}](z(t))\tilde{a}\end{aligned} \quad (15)$$

where $[L_{(i,j)} v_b]$ is the vector of filtered signals with different Laguerre bases $[[L_i v_b], [L_{i-1} v_b], \ldots, [L_j v_b]], i \geq j$, and $\tilde{a} = \begin{bmatrix}\tilde{a}_1 & \tilde{a}_2\end{bmatrix}^\top, \tilde{b} = \begin{bmatrix}\tilde{b}_0 & \tilde{b}_1 & \tilde{b}_2\end{bmatrix}^\top$ are vectors of the model parameters. $\tilde{a}_i, \tilde{b}_j$ are defined as $\tilde{a}_i := \bar{a}_i/\bar{a}_0, \tilde{b}_j := \bar{b}_j/\bar{b}_0$. In this formulation, we assume that $\bar{a}_0 \neq 0$, which can be satisfied for a properly defined system and a suitable ν, followed by (8).

B. Cubic B-spline for modeling the OCV-SOC relation

Since the OCV v_{oc} is not directly measurable and exhibits significantly different behaviors across different regions of SOC, we model it with a cubic B-spline function. A B-spline is a piecewise polynomial that enables local control of the estimated curve [14]. The shape-preserving property of the B-spline suits better our OCV identification than traditional polynomial basis functions. To model the OCV as a cubic B-spline, we write v_{oc} as:

$$v_{oc}(z(t)) = \sum_{i=1}^{h} \gamma_i g_i(z(t)) \quad (16)$$

where g_i are the B-spline basis functions, γ_i are the control points, and h is the number of bases. The basis function is defined over a non-decreasing knot vector $Z := [z_0, \ldots, z_{h+3}]$, where $z_0 \leq \cdots \leq z_{h+3}$ are the positions of the splines knots. Define $p \in \mathbb{Z}_{\geq 0}$ the degree of B-spline. Then, the value of the basis functions can be computed recursively via the de Boor-Cox formula [15] as:
for $p > 0$:

$$\begin{aligned}g_{i,p}(z(t)) = &\frac{z(t) - z_i}{z_{i+p} - z_i} g_{i,p-1}(z(t)) + \\ &\frac{z_{i+p+1} - z(t)}{z_{i+p+1} - z_{i+1}} g_{i+1,p-1}(z(t));\end{aligned} \quad (17)$$

for $p = 1$:

$$g_{i,0}(z(t)) = \begin{cases} 1 & \text{if } z_i \leq z(t) < z_{i+1} \\ 0 & \text{otherwise}\end{cases}. \quad (18)$$

In our case, $p = 3$ for the cubic B-spline. A p-th degree B-spline has a $(p-1)$-th order continuity, with the p-th order derivative being a piecewise constant function. The d-th order derivative of the basis of B-spline can be computed as:

$$\begin{aligned}s_{i,p}^{(d)}(z(k)) = &\frac{p}{z_{i+p} - z_i} s_{i,p-1}^{(d-1)}(z(k)) - \\ &\frac{p}{z_{i+p+1} - z_{i+1}} s_{i+1,p-1}^{(d-1)}(z(k))\end{aligned} \quad (19)$$

We will use the derivative of the cubic B-spline in a sequel for knot selection.

With the cubic B-spline (16) for modeling the v_{oc}, we can write the Laguerre filtered version of v_{oc} used in (11) as:

$$[L_k v_{oc}](z(t)) = \sum_{i=1}^{h} \gamma_i [L_k g_i](z(t)),\ k = 0, 1, 2. \quad (20)$$

This corresponds to applying the Laguerre filter to individual bases of the cubic B-spline. Then, we rewrite the regression model (15) with cubic B-spline bases as:

$$\begin{aligned}[L_2 v_b](t) = \begin{bmatrix}-[L_{(1,0)} v_b](t) & [L_{(2,0)} i_b](t)\end{bmatrix}\begin{bmatrix}\tilde{a} \\ \tilde{b}\end{bmatrix} + \\ [L_2 g](z(t))\gamma + [L_{(1,0)} g](z(t))\tilde{a}(\gamma)\end{aligned} \quad (21)$$

where $g(z(t)) := [g_1(z(t)), \ldots, g_h(z(t))] \in \mathbb{R}^h$ is a vector of B-spline bases, and $[L_k g]$ denotes applying the Laguerre filter L_k to individual elements of g. $\gamma := [\gamma_1, \ldots, \gamma_h]^\top \in \mathbb{R}^h$ represents the vector of B-spline control points. $\tilde{a}(\gamma) \in \mathbb{R}^{2h}$ is a bilinear vector of $\tilde{a}$ and γ:

$$\tilde{a}(\gamma) := \tilde{a} \otimes \gamma = \begin{bmatrix}\tilde{a}_1\gamma \\ \tilde{a}_2\gamma\end{bmatrix}, \quad (22)$$

where $\otimes$ is the Kronecker product.

From the formulation of the regression model (21), we can write a data equation for the ECM as:

$$\begin{aligned}[L_2 V_b]_m = \begin{bmatrix}-[L_{(1,0)} V_b]_m & [L_{(2,0)} I_b]_m & [L_2 G]_m\end{bmatrix}\begin{bmatrix}\tilde{a} \\ \tilde{b} \\ \gamma\end{bmatrix} + \\ [L_{(1,0)} G]_m \tilde{a}(\gamma)\end{aligned} \quad (23)$$

where $[L_{(1,0)}V_b]_m \in \mathbb{R}^{(m+1)\times 2}$ is the data matrix:

$$[L_{(1,0)}V_b]_m = \begin{bmatrix} [L_{(1,0)}v_b](t_0) \\ \vdots \\ [L_{(1,0)}v_b](t_m) \end{bmatrix}, \tag{24}$$

and $[L_{(2,0)}I_b]_m \in \mathbb{R}^{(m+1)\times 3}$, $[L_{(1,0)}G]_m \in \mathbb{R}^{(m+1)\times 2h}$ are similarly defined. $t_i := iT_s$ is the time instant of the i-th sample and $T_s > 0$ is the sampling time. With (23), we can write the following least squares problem to identify the battery parameters and the B-spline control points:

$$\min_{\varphi,\tilde{a}(\gamma)} \left\| [L_2V_b]_m - \Phi\varphi - [L_{(1,0)}G]_m\tilde{a}(\gamma) \right\|_F^2 \tag{25}$$

where $\Phi \in \mathbb{R}^{(m+1)\times(2+3+h)}$ is the data matrix:

$$\Phi = \begin{bmatrix} -[L_{(1,0)}V_b]_m & [L_{(2,0)}I_b]_m & [L_2V_{oc}]_m \end{bmatrix}, \tag{26}$$

and $\varphi = [\tilde{a}^\top, \tilde{b}^\top, \gamma^\top]^\top \in \mathbb{R}^{2+3+h}$ are the parameters of the transfer function and the coefficients of the cubic B-spline. Since $\tilde{a}(\gamma)$ (22) is the Kronecker product between $\tilde{a}$ and γ, (25) is a bilinear optimization problem that is generally expensive to solve due to nonconvexity [16]. To impose the bilinear structure in $\tilde{a}(\gamma)$, we exploit the property that the matrix $P = \begin{bmatrix} M & \tilde{a} \\ \gamma^\top & 1 \end{bmatrix} \in \mathbb{R}^{3\times(h+1)}$, where $M := \tilde{a}\gamma^\top \in \mathbb{R}^{2\times h}$ has a rank of one:

$$\operatorname{rank}\left(\begin{bmatrix} M & \tilde{a} \\ \gamma^\top & 1 \end{bmatrix} \right) = 1. \tag{27}$$

The matrix M is formulated from the bilinear term $\tilde{a}(\gamma)$ using $\tilde{a}(\gamma) = \operatorname{vec}(M)$, where $\tilde{a}(\gamma)$ is a row-wise vectorization of M. To impose the low-rank property of P, we regularize its nuclear norm, which is a convex relaxation of the rank computation. With the low-rank regularization, we formulated the bilinear optimization problem (25) into the following rank regularized least squares problem:

$$\min_{\varphi,\tilde{a}(\gamma)} \left\| [L_2V_b]_m - \Phi\varphi - [L_{(1,0)}G]_m\tilde{a}(\gamma) \right\|_F^2 + \lambda_1\|P\|_* \tag{28}$$

where $\|\cdot\|_*$ is the nuclear norm and $\lambda_1 \in \mathbb{R}_{\geq 0}$ is the regularization coefficient.

To mitigate overfitting to measurement noise in cubic B-splines, we reduce the number of knots by selecting knots where a high variation of the spline is required. This can be achieved by using the property that the third-order derivative of the cubic B-spline is a piecewise constant function, and the discontinuities occur at the knot places [14], as illustrated in Figure 2. To select knot positions, we regularize the sparsity of the finite difference of the third-order derivatives of cubic splines by using an L1 regularization in (28). This results in the following rank and L1 regularized least squares problem:

$$\min_{\varphi,\tilde{a}(\gamma)} \left\| [L_2V_b]_m - \Phi\varphi - [L_{(1,0)}G]_m\tilde{a}(\gamma) \right\|_F^2 + \lambda_1\|P\|_* + \lambda_2\|\mathcal{D}G_m^{(3)}\gamma\|_1 \tag{29}$$

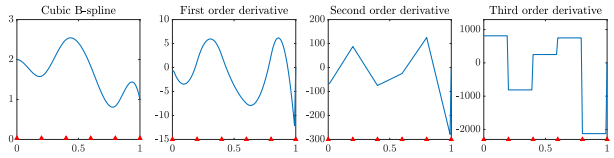

Fig. 2. Cubic B-spline and its first to third-order derivatives. Knot places represented by red triangles mark the derivatives' discontinuities

where $G_m^{(3)}$ is the derivatives of the cubic B-spline bases:

$$G_m^{(3)} = \begin{bmatrix} g_1^{(3)}(z_0) & \cdots & g_h^{(3)}(z_0) \\ g_1^{(3)}(z_1) & \cdots & g_h^{(3)}(z_1) \\ \vdots & \ddots & \vdots \\ g_1^{(3)}(z_m) & \cdots & g_h^{(3)}(z_m) \end{bmatrix}, \tag{30}$$

$g_i^{(3)}$ is the third-order derivative of g_i computed by (19), and $\mathcal{D} \in \mathbb{R}^{m\times(m+1)}$ is a finite difference matrix:

$$\mathcal{D} = \begin{bmatrix} 1 & -1 & & \\ & \ddots & \ddots & \\ & & 1 & -1 \end{bmatrix}. \tag{31}$$

In (30), the sequence $\{z_i\}$ is a sorted SOC, where $z_i \leq z_{i+1}, i = 0, 1, \ldots, m-1$, to ensure that the finite difference is computed over a monotonic SOC instead of time [4]. By reducing the L1 norm, we can achieve a sparse solution in the discontinuities of the third-order derivative of the cubic B-spline, thus revealing the necessary variation of the B-spline to represent the OCV-SOC curve [17].

With the parameters $\tilde{a}, \tilde{b}$ identified by solving (29), we can find the transfer function coefficients a_i, b_j in (4) by solving equations using (8)-(10), and $\tilde{a}_i = \bar{a}_i/\bar{a}_0, \tilde{b}_j = \bar{b}_j/\bar{a}_0$ for $i = 1, 2, j = 0, 1, 2$. Then, the physical parameters of the battery can be retrieved using the following relations:

$$\begin{aligned} a_1 &= \frac{1}{R_1C_1} + \frac{1}{R_2C_2}, \; a_2 = \frac{1}{R_1C_1R_2C_2}, \; b_0 = R_0, \\ b_1 &= R_0\left(\frac{1}{R_1C_1} + \frac{1}{R_2C_2}\right) + \frac{1}{C_1} + \frac{1}{C_2}, \\ b_2 &= \frac{R_0 + R_1 + R_2}{R_1C_1R_2C_2} \end{aligned} \tag{32}$$

In the next section, we evaluate the effectiveness of the developed method for battery identification and OCV-SOC reconstruction on a simulated battery and real-life data.

IV. Numerical Experiments With Simulated and Real-Life Battery Data

We first validate the efficacy of the developed method by a simulated battery. Then, we apply this approach to real-life battery data from [12].

A. Validation on a simulated battery

The simulated battery is built with parameters shown in Table I, where the different time constants $\tau_1 = 18$s and $\tau_2 = 100$s are used to validate the performance of the developed method for identifying a fast and a slow dynamic of the battery.

TABLE I

RESISTORS (Ω) AND CAPACITORS (F) OF THE SIMULATED BATTERY

Parameters	R_0	R_1	R_2	C_1	C_2
Values	0.06	0.03	0.02	600	5000

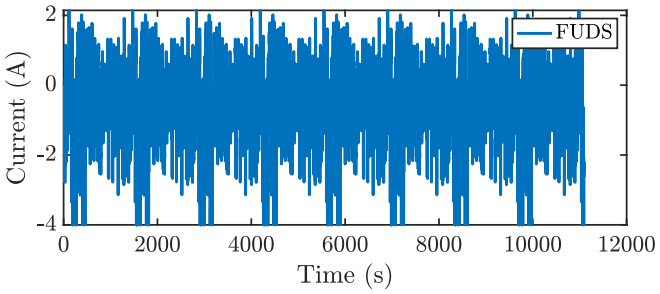

Fig. 3. Federal Urban Driving Schedule Profile

The OCV-SOC curve emulating experimental OCV data [7] is simulated with the following function:

$$v_{oc}(z(t)) = 3 + 0.03(1.5 - z(t))^{-4} + 0.1\log(z(t) + 0.01).$$

The input to the simulated battery shown in Figure 3 is the FUDS profile designed to emulate the real-life driving conditions of EVs. The output of the simulated battery is contaminated by white noise with a standard deviation $\sigma = 10^{-4}$ to emulate measurement noise. Monte Carlo simulations with 20 different noise realizations are applied to evaluate the performance of the developed method.

We solve the rank and L1 regularized least squares (29) using data from the simulated battery to identify the battery parameters. The cut-off frequency of the Laguerre filter is $1e-3$, and the number of knots of the B-splines is 21. The optimization problem is solved in MATLAB by `cvx` toolbox [18] with Mosek solver [19]. The performance of the identified model is evaluated with root mean squares error (RMSE) and variance-account-for (VAF) [20] defined by:

$$V_{RMSE} = \sqrt{\frac{\sum_{i=0}^{m}(v_b(t_i) - \hat{v}_b(t_i))^2}{n}}, \tag{33}$$

$$VAF = \left(1 - \frac{\text{var}(v_b(t_i) - \hat{v}_b(t_i))}{\text{var}(v_b(t_i))}\right) \times 100\%, \tag{34}$$

where v_b is the measured or simulated battery voltage and $\hat{v}_b$ is the estimated value of the model.

The regularization coefficients λ_1, λ_2 for the nuclear norm and L1 norm are determined by using grid search on the coefficient space. We selected the coefficients that yield the minimum RMSE in solving the regularized least squares problem (29). The selected coefficients with minimum RMSE are $\lambda_1 = 2e-06$, $\lambda_2 = 1e-08$.

With these coefficients, the fitting of the identified model to the simulated data is shown in Figure 4. The RMSE of the model is 0.29 mV, and the VAF is 99.74%. The identified parameters of 20 Monte Carlo simulations are shown in Figure 5. The figure indicates that the estimated parameters are generally consistent with the actual values. The OCV-SOC identification is shown in Figure 6. The estimated OCV curve is aligned with the actual value with a mild deviation. The results of the simulated data demonstrate the effectiveness of the developed method in jointly identifying the battery parameters and the OCV-SOC curve. The physical parameters with distinct time constants can also be successfully identified.

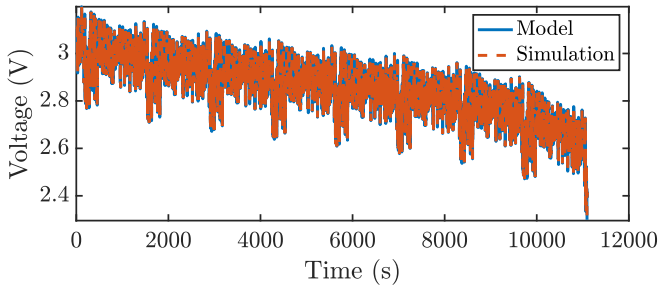

Fig. 4. Model output in comparison with the simulated output

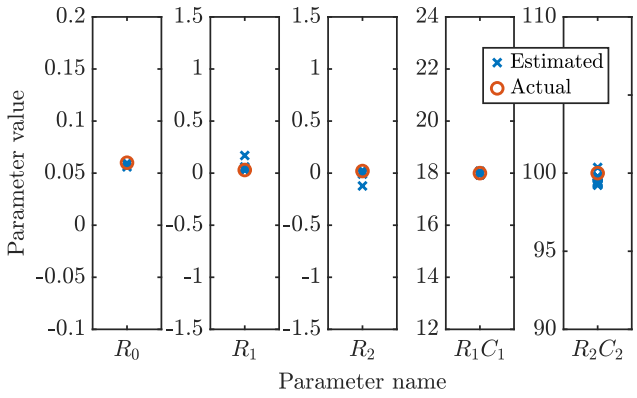

Fig. 5. Estimated battery parameters in comparison to the actual values

B. Application to real-life battery data

With the efficacy validated via the simulated battery, we apply the developed method to real-life battery data. We used the data from the CALCE dataset [12]. The studied battery is discharged with the FUDS profile at a temperature of 25°C and 80% initial SOC. The OCV-SOC curve of the battery is measured under the incremental OCV test to validate the OCV-SOC identification.

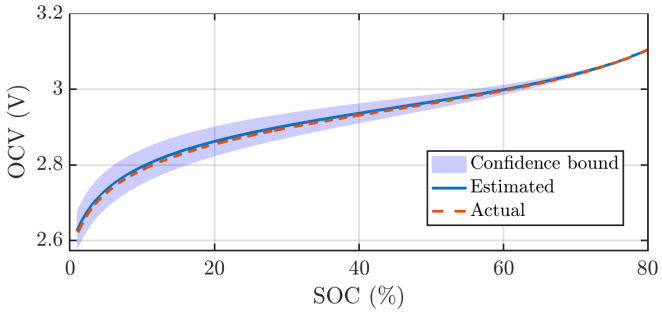

Fig. 6. Estimated OCV-SOC mapping with 2σ standard deviation bounds in comparison to the actual values

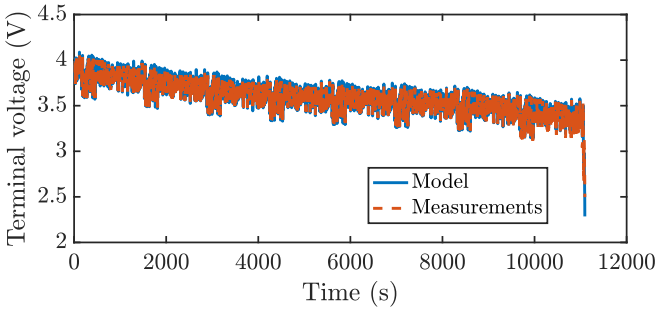

Fig. 7. Model output in comparison with the measured voltage

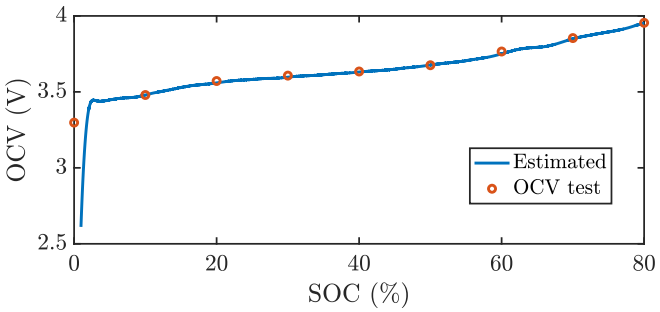

Fig. 8. Estimated OCV-SOC mapping in comparison with the results of the OCV test

The regularization coefficients are $\lambda_1 = 1.67e-06$, $\lambda_2 = 1.00e-08$, determined by conducting a grid search as applied in the simulated battery. The voltage fitting of the identified model is shown in Figure 7. The RMSE of the voltage fit is 0.0156V, and the VAF of the model is 99.3522%. The identified battery parameters are shown in Table II. The time constants of the tested battery are 1.55s and 30.94s, indicating the fast-slow dynamics of the battery.

The reconstructed OCV-SOC curve is pictured in Figure 8. From the figure, we see that the identified OCV is aligned with the OCV test, and the estimated curve provides more details about the OCV during intervals between OCV samples, especially in the range from 60% to 70%. The drastic decrease of the OCV within 0% to 10% SOC indicates a large voltage drop of the battery when approaching depletion. This information cannot be attained from the battery OCV tests but is feasible by direct estimation of the OCV-SOC relation. The validated result illustrates the advantages of directly identifying the OCV-SOC relation from the dynamic data over conducting OCV tests.

TABLE II

IDENTIFIED RESISTORS [Ω] AND CAPACITORS [F] VALUES OF THE TESTED BATTERY

Parameters	R_0	R_1	R_2	C_1	C_2
Values	0.0648	0.0105	0.0158	147.9061	1958.39

V. CONCLUSION

We developed a continuous-time method to jointly identify battery parameters and the OCV-SOC relation from dynamic data. Laguerre filters were utilized to achieve continuous-time identification, and the OCV-SOC relation was modeled using a cubic B-spline to represent the piecewise nonlinearity. Battery parameters and the OCV curve are jointly identified by solving a rank and L1 regularized least squares problem. Simulated and real-life data validate the effectiveness of the developed method. Future work will account for variable battery parameters.

REFERENCES

[1] M. A. Hannan, M. H. Lipu, A. Hussain, and A. Mohamed, "A review of lithium-ion battery state of charge estimation and management system in electric vehicle applications: Challenges and recommendations," *Renewable and Sustainable Energy Reviews*, vol. 78, pp. 834–854, 2017.

[2] G. L. Plett, *Battery management systems, Volume I: Battery modeling*, vol. 1. Artech House, 2015.

[3] J. Tian, X. Liu, S. Li, Z. Wei, X. Zhang, G. Xiao, and P. Wang, "Lithium-ion battery health estimation with real-world data for electric vehicles," *Energy*, vol. 270, p. 126855, 2023.

[4] Y. Wang, R. M. Ferrari, and M. Verhaegen, "Concurrent li-ion battery parameter estimation and open-circuit voltage reconstruction via l1-regularized least squares," in *2024 European Control Conference (ECC)*, pp. 3551–3556, IEEE, 2024.

[5] J. Li, Y. Wang, R. M. Ferrari, J. Swevers, and F. Ding, "Online lithium-ion battery modeling and state of charge estimation via concurrent state and parameter estimation," *IFAC-PapersOnLine*, vol. 58, no. 15, pp. 462–467, 2024.

[6] B. Haverkamp, M. Verhaegen, C. Chou, and R. Johansson, "Continuous-time subspace model identification method using laguerre filtering," *IFAC Proceedings Volumes*, vol. 30, no. 11, pp. 1093–1098, 1997.

[7] Z. Yang and X. Wang, "An improved parameter identification method considering multi-timescale characteristics of lithium-ion batteries," *Journal of Energy Storage*, vol. 59, p. 106462, 2023.

[8] C. T. Chou, M. Verhaegen, and R. Johansson, "Continuous-time identification of siso systems using laguerre functions," *IEEE Transactions on Signal Processing*, vol. 47, no. 2, pp. 349–362, 1999.

[9] R. Johansson, "Identification of continuous-time models," *IEEE Transactions on Signal Processing*, vol. 42, no. 4, pp. 887–897, 1994.

[10] M. Chen and G. A. Rincon-Mora, "Accurate electrical battery model capable of predicting runtime and iv performance," *IEEE transactions on energy conversion*, vol. 21, no. 2, pp. 504–511, 2006.

[11] B. Xia, X. Zhao, R. De Callafon, H. Garnier, T. Nguyen, and C. Mi, "Accurate lithium-ion battery parameter estimation with continuous-time system identification methods," *Applied energy*, vol. 179, pp. 426–436, 2016.

[12] F. Zheng, Y. Xing, J. Jiang, B. Sun, J. Kim, and M. Pecht, "Influence of different open circuit voltage tests on state of charge online estimation for lithium-ion batteries," *Applied energy*, vol. 183, pp. 513–525, 2016.

[13] M. Shokri, L. Lyons, S. Pequito, and L. Ferranti, "Battery identification with cubic spline and moving horizon estimation for mobile robots," *IEEE Transactions on Control Systems Technology*, 2024.

[14] R. Yeh, Y. S. Nashed, T. Peterka, and X. Tricoche, "Fast automatic knot placement method for accurate b-spline curve fitting," *Computer-aided design*, vol. 128, p. 102905, 2020.

[15] X. Ma and W. Shen, "Generalized de boor–cox formulas and pyramids for multi-degree spline basis functions," *Mathematics*, vol. 11, no. 2, p. 367, 2023.

[16] J. Noom, O. Soloviev, and M. Verhaegen, "Proximal-based recursive implementation for model-free data-driven fault diagnosis," *Automatica*, vol. 165, p. 111656, 2024.

[17] R. Mustata, M. Verhaegen, H. Ohlsson, and F. Gustafsson, "Receding horizon estimation of arbitrarily changing unknown inputs," *IFAC Proceedings Volumes*, vol. 47, no. 3, pp. 5939–5944, 2014.

[18] M. Grant and S. Boyd, "Cvx: Matlab software for disciplined convex programming, version 2.1," 2014.

[19] M. ApS, *The MOSEK optimization toolbox for MATLAB manual. Version 10.0.*, 2022.

[20] M. Verhaegen and V. Verdult, *Filtering and system identification: a least squares approach*. Cambridge university press, 2007.